



# A direct method to predict cyclic steady states of elastoplastic structures

Konstantinos V. Spiliopoulos\*, Konstantinos D. Panagiotou

*Institute of Structural Analysis & Antiseismic Research, Department of Civil Engineering, National Technical University of Athens, Zografou Campus, 157-80 Athens, Greece*

## ARTICLE INFO

### Article history:

Received 1 December 2011

Received in revised form 3 February 2012

Accepted 5 March 2012

Available online 13 March 2012

### Keywords:

Direct methods

Cyclic loading

Fourier series

Elastic shakedown

Alternating plasticity

Ratcheting

## ABSTRACT

The asymptotic steady state behavior of an elastic–perfectly plastic structure under cyclic loading may be determined by time consuming incremental time-stepping calculations. Direct methods, alternatively, have a big computational advantage as they attempt to find the characteristics of the cyclic state right from the start of the calculations. Most of these methods address an elastic shakedown state through the shakedown theorems and on the basis of mathematical programming algorithms. In the present paper, a novel direct method that has a more physical basis and may predict any cyclic stress state of a structure under a given loading is presented. The method exploits the cyclic nature of the expected residual stress distribution at the steady cycle. Thus, after equilibrating the elastic part of the total stress with the external load, the unknown residual stress part is decomposed into Fourier series whose coefficients are evaluated iteratively by satisfying compatibility and equilibrium with zero loads at time points inside the cycle and then integrating over the cycle. A computationally simple way to account for plasticity is proposed. The procedure converges uniformly to the true cyclic residual stress for a loading below the elastic shakedown limit or to an unsafe cyclic total stress, which may be used to mark the regions with plastic straining inside the cycle. The method then continues to determine whether the applied loading would lead the structure to ratcheting or to regions that alternate plastically. The procedure is formulated within the finite element method. A von Mises yield surface is typically used. Examples of application of one and two dimensional structures are included.

© 2012 Elsevier B.V. All rights reserved.

## 1. Introduction

Structures, subjected to elevated repeated thermo-mechanical loading, are, nowadays forced to operate beyond their elastic limit. The integrity assessment of such structures is an important task for the structural engineer. Examples of structures, operating under such loading conditions may be found in mechanical engineering, like pressure vessels, aircraft gas propulsion engines, general machinery. In civil engineering such situations arise in constructions like dams, pavements, offshore platforms, buildings and bridges under seismic actions.

The complete response of a structure, which is subjected to a given thermo-mechanical loading and exhibits inelastic time independent plastic strains, is quite complex. The reason of the complexity is the need to perform calculations over the lifetime history of the structure. The computation of the whole loading history, however, leads to lengthy and expensive incremental calculations, especially for structures with a high degree of redundancy. Therefore, it is very useful to develop computational approaches for straightforward calculations of the possible stabilized state under repeated thermo-mechanical loading.

Direct methods offer this alternative. Based on the fact that for scleronomic or rheonomic stable materials [1] such a stabilized cyclic state exists, they search for this asymptotic state right from the start of the calculations.

The most well known cyclic state is the elastic shakedown. The search for this state is based on the lower [2] and upper bound [3] shakedown theorems of plasticity. Although originally for elastic–perfectly plastic material behavior and first order theory, extensions were made to cater for hardening and second-order effects [4], as well as for dynamic loadings [5]. More recently, the theorems were extended to structures with poroplastic material behavior [6].

The formulation of these problems is normally done using mathematical programming (MP). Efficient procedures like a non-linear Newton-type algorithm [7] or the interior point methods (IPM) (e.g. [8–10]) are employed to estimate the shakedown load factor, with various applications to engineering problems (e.g. [11,12]).

Recently Garcea and Leonetti [13], within the MP formulation, arc length techniques have been used instead of the IPMs.

Much fewer approaches that are not based on MP also exist in the literature. One such approach uses internal variables each of which correspond to an inelastic mechanism (e.g. [14,15]). A more recent procedure, which has a better physical understanding, is the Linear Matching Method (LMM), originally introduced in [16].

\* Corresponding author. Tel.: +30 210 7721603; fax: +30 210 7721604.

E-mail address: [kvspilio@central.ntua.gr](mailto:kvspilio@central.ntua.gr) (K.V. Spiliopoulos).

The method is a generalization of the elastic compensation method ([17,18]) and is based on matching a linear problem to a plasticity problem. A sequence of linear solutions, with a spatially varying moduli, are generated that provide upper bounds that monotonically converge to the least upper bound, which coincides with the collapse load [19] or the shakedown load [20].

The method was further extended beyond shakedown, both theoretically [21] and numerically [22], to provide an upper bound estimation of the ratchet boundary for a loading that can be decomposed into constant and time varying components. Recently, to approach this boundary, an addition of a lower bound calculation to the LMM upper bound ratchet analysis was proposed [23]. A numerical procedure, based also on the splitting of constant and time varying loading was presented in [24,25]. Recently also, a simplified method to find the ratchet boundary was suggested [26], based on the fictitious yield surface proposed in [27].

Although important to find this boundary, it is equally important to be able to determine the long-term effects that a given cyclic loading will have on the structure. To this end, an alternative to the cumbersome incremental procedure, a method called Direct Cycle Analysis (DCA) has been suggested in [28] and has been implemented in the commercial program Abaqus [29]. This method is based on assuming that the displacements at the steady cycle will become cyclic. One then proceeds to decompose them into Fourier series whose coefficients are evaluated in an iterative way by linking them with the coefficients of the Fourier series of the residual load vector. This vector is evaluated as in an incremental procedure, and static admissibility is enforced by leading it to zero. The procedure, although involved, appears to be suited for the cases of alternating plasticity but fails to converge for loadings that are close to ratcheting [29], as, due to the assumed cyclic displacement behavior, has the inherent inability to predict such a case.

The present work proposes a Direct Method that may be used to estimate the long-term behavior of an elastic–perfectly plastic structure under a given cyclic loading. It has its roots on a simplified way to predict creep cyclic stress states [30,31]. The method addresses the physics of the steady cycle which furnishes the cyclic nature of the residual stresses. It may be called the Residual Stress Decomposition Method (RSDM) and is based on decomposing the expected residual stresses in Fourier series inside the cycle of loading. The coefficients of the Fourier series are evaluated in an iterative way by integrating the residual stress rates over the cycle. These rates have been found by satisfying equilibrium and compatibility at time points inside the cycle. Plastic straining is accounted for in a novel way by adding the elastic and the residual stress at the cycle points. If the sum exceeds the yield surface, the plastic strain rate effect is estimated through the stress in excess of the yield surface. These stresses provide then input, as equivalent nodal forces, for iteration. When the plastic strain rates stabilize, in the form of a converged residual stress vector, the procedure stops. Any of the three different cases, shakedown, alternating plasticity or ratcheting, may, equally easily, be realized. The procedure is applied to a typical one and a two dimensional structure subjected to different loading cases. Results show a stable and computationally efficient procedure with uniform convergence characteristics.

## 2. Cyclic stress state

Consider a body of volume  $V$  and surface area  $S$ . Let us assume that on a part of  $S$  zero displacement conditions are applied and on another part of  $S$  the structure is subjected to a mechanical loading, of the form:

$$\mathbf{P}(t) = \mathbf{P}(t + nT), \tag{1}$$

where  $\mathbf{P}(t) = \{P_1(t), P_2(t), \dots, P_n(t)\}$ ;  $t$  is a time point inside a cycle,  $T$  is the period of the cycle,  $n = 1, 2, \dots$ , denotes number of full cycles.

Such a loading constitutes a cyclic loading state. A loading trajectory of such a state in a two dimensional loading domain may be seen in Fig. 1.

Let us suppose that our structure is made of an elastic–perfectly plastic material. Concentrating at a particular time point  $\tau = \frac{t}{T}$  inside the cycle, the structure develops a stress field  $\sigma_{ij}(\tau)$  that may be decomposed in two parts: one, assuming a completely linear elastic material behavior, denoted by  $\sigma_{ij}^{el}(\tau)$ , which equilibrates the external loading and one which is a self-equilibrating residual stress system  $\rho_{ij}(\tau)$ , due to inelasticity. Thus one may write:

$$\sigma_{ij}(\tau) = \sigma_{ij}^{el}(\tau) + \rho_{ij}(\tau). \tag{2}$$

At the same time, the corresponding strain rates may also be decomposed into two parts:

$$\dot{\epsilon}_{ij}(\tau) = \dot{\epsilon}_{ij}^{el}(\tau) + \dot{\epsilon}_{ij,r}(\tau). \tag{3}$$

The residual strain rate  $\dot{\epsilon}_{ij,r}(\tau)$  consists not only of the plastic strain rates  $\dot{\epsilon}_{ij}^{pl}(\tau)$  but also of an elastic strain rate part  $\dot{\epsilon}_{ij,r}^{el}(\tau)$  which is necessary so that total strain compatibility is maintained. Thus Eq. (3) may be written as:

$$\dot{\epsilon}_{ij}(\tau) = \dot{\epsilon}_{ij}^{el}(\tau) + \dot{\epsilon}_{ij,r}^{el}(\tau) + \dot{\epsilon}_{ij}^{pl}(\tau). \tag{4}$$

The first two strain rate components are given in terms of their corresponding stress rates, where differentiation is meant with respect to  $\tau$ . For the third component, i.e. the plastic strain rate, an associated flow rule with a yield surface  $f$  has been assumed:

$$\begin{aligned} \dot{\epsilon}_{ij}^{el}(\tau) &= C_{ijkl} \dot{\sigma}_{kl}^{el}(\tau), \\ \dot{\epsilon}_{ij,r}^{el}(\tau) &= C_{ijkl} \dot{\rho}_{kl}(\tau), \\ \dot{\epsilon}_{ij}^{pl}(\tau) &= \lambda \frac{\partial f}{\partial \sigma_{ij}(\tau)} \end{aligned} \tag{5}$$

with  $C_{ijkl}$  the tensor of elastic constants.

Based on the convexity of the yield surface (Fig. 2), two states of stress and their corresponding plastic strain rates obey Drucker's postulate for stable materials:

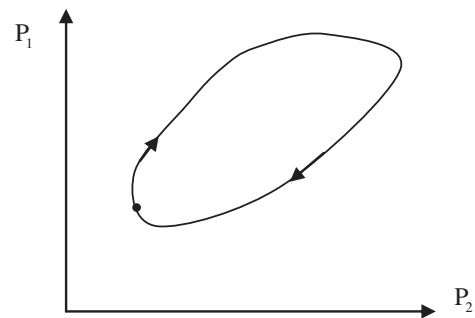


Fig. 1. Cyclic loading state.

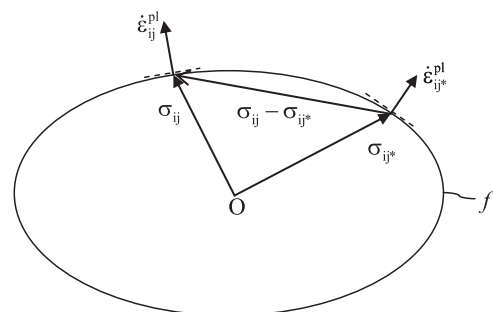


Fig. 2. Corresponding pairs of stresses and plastic strain rates on convex yield surface.

$$(\sigma_{ij} - \sigma_{ij}^*) \dot{\epsilon}_{ij}^{pl} \geq 0 \quad (\sigma_{ij}^* - \sigma_{ij}) \dot{\epsilon}_{ij}^{pl} \geq 0. \tag{6}$$

It may be proved [32] that under the loading described above and for such a material behavior, Drucker's postulate leads to the existence of a steady cycle in which the stresses and the strain rates gradually stabilize and remain unaltered on passing to the next cycle [27]. Thus the stresses and strain rates become periodic having the same period  $T$  with the loading [33]. This cyclic state, in a real structure, will be reached after the application of many cycles.

The evolution of a simple uniaxial cyclic straining (Fig. 3) reveals each of the three different possible asymptotic states that have been classified in [34]:

- (a) For relative low load amplitudes, the structure *shakes down* elastically, i.e. the behavior appears to be purely elastic (Fig. 3(a)). This may be asymptotically described by:

$$\dot{\epsilon}_{ij}^{pl,cs} = \lim_{n \rightarrow \infty} \dot{\epsilon}_{ij}^{pl}(\tau) = 0, \tag{7}$$

where *cs* stands for cyclic steady state.

- (b) For certain patterns and levels of loading, plastic strain increments appear to be alternating in sign over the cycle and tend to cancel each other, thus the total deformation remains low. This phenomenon is called *alternating or reverse plasticity* and failure may occur due to low-cycle fatigue (Fig. 3(b)). This asymptotically may be described as:

$$\begin{aligned} \dot{\epsilon}_{ij}^{pl,cs}(\tau) &= \lim_{n \rightarrow \infty} \dot{\epsilon}_{ij}^{pl}(\tau) \neq 0, \\ \Delta \epsilon_{ij}^{pl,cs} &= \int_0^1 \dot{\epsilon}_{ij}^{pl,cs}(\tau) d\tau = 0. \end{aligned} \tag{8}$$

- (c) For certain patterns and levels of loading, the plastic strain increments in each load cycle are of the same sign resulting to total strains and thus displacements to be large so that the structure becomes unserviceable. This situation is called *incremental collapse or ratcheting* (Fig. 3(c)). The asymptotic behavior is described by:

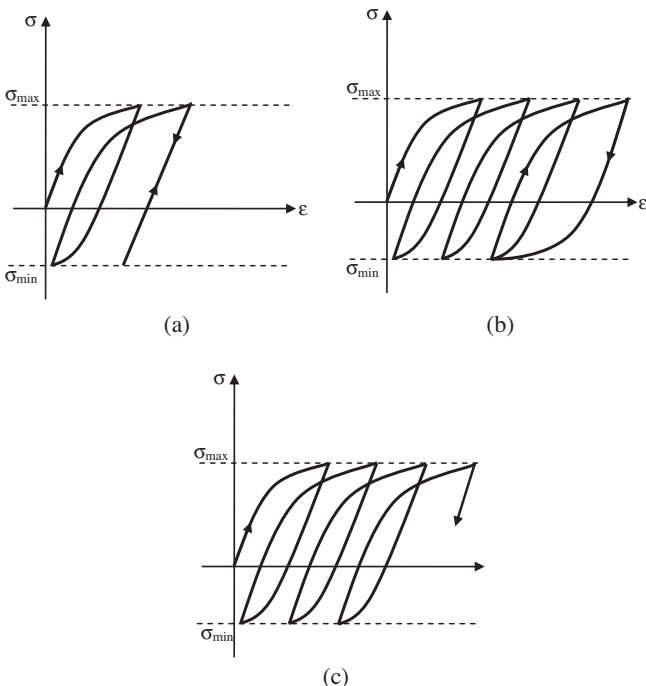


Fig. 3. (a) Shakedown, (b) alternating plasticity and (c) incremental collapse.

$$\begin{aligned} \dot{\epsilon}_{ij}^{pl,cs}(\tau) &= \lim_{n \rightarrow \infty} \dot{\epsilon}_{ij}^{pl}(\tau) \neq 0, \\ \Delta \epsilon_{ij}^{pl,cs} &= \int_0^1 \dot{\epsilon}_{ij}^{pl,cs}(\tau) d\tau \neq 0. \end{aligned} \tag{9}$$

Another consequence of the Drucker's postulate is that the stress distribution in the steady cycle does not depend upon any initial condition, prior to the first cycle, and is unique in those regions where we have non-vanishing plastic strain rates ([27,33]).

### 3. Residual stress decomposition

Since the total stress  $\sigma_{ij}(\tau)$  will, asymptotically, become cyclic, and the elastic stress  $\sigma_{ij}^{el}(\tau)$ , that equilibrates the cyclic loading, is obviously also cyclic, the residual stress  $\rho_{ij}(\tau)$  will become also cyclic. Thus one may decompose them in Fourier series. We may write (see, for example, [35]):

$$\rho_{ij}(\tau) = \frac{a_{0,ij}}{2} + \sum_{k=1}^{\infty} (a_{k,ij} \cos 2k\pi\tau + b_{k,ij} \sin 2k\pi\tau). \tag{10}$$

Thus to determine the residual stress distribution one has to evaluate the various Fourier coefficients of (10).

If we differentiate (10) we get:

$$\dot{\rho}_{ij}(\tau) = 2\pi \sum_{k=1}^{\infty} \{(-ka_{k,ij}) \sin 2k\pi\tau + kb_{k,ij} \cos 2k\pi\tau\}. \tag{11}$$

Expanding Eq. (11) we may get:

$$\begin{aligned} \dot{\rho}_{ij}(\tau) &= 2\pi \{-a_{1,ij} \sin 2\pi\tau + (-2a_{2,ij}) \sin 4\pi\tau + \dots + (-ka_{k,ij}) \\ &\quad \times \sin 2k\pi\tau + b_{1,ij} \cos 2\pi\tau + (2b_{2,ij}) \cos 4\pi\tau + \dots \\ &\quad + (kb_{k,ij}) \cos 2k\pi\tau\}. \end{aligned} \tag{12}$$

If we multiply (12) by  $\sin 2k\pi\tau$  and then integrate over a cycle, using the orthogonality properties of the trigonometric functions, we may find that a typical coefficient of the cosine series is given by:

$$a_{k,ij} = -\frac{1}{k\pi} \int_0^1 \{\dot{\rho}_{ij}(\tau)\}(\sin 2k\pi\tau) d\tau. \tag{13}$$

If now we multiply (12) by  $\cos 2k\pi\tau$  and carry over the same procedure we get for a coefficient of the sine series:

$$b_{k,ij} = \frac{1}{k\pi} \int_0^1 \{\dot{\rho}_{ij}(\tau)\}(\cos 2k\pi\tau) d\tau. \tag{14}$$

On the other hand, if we integrate (11) over a cycle, we get the following expression:

$$\begin{aligned} \int_0^1 \dot{\rho}_{ij}(\tau) d\tau &= \rho_{ij}(1) - \rho_{ij}(0) = \left(\frac{a_{0,ij}}{2}(1) + \sum_{k=1}^{\infty} a_{k,ij}(1)\right) \\ &\quad - \left(\frac{a_{0,ij}}{2}(0) + \sum_{k=1}^{\infty} a_{k,ij}(0)\right), \end{aligned} \tag{15}$$

where Eq. (10) at the beginning and at the end of the cycle was used. With all the coefficients known at the beginning of the cycle and the coefficients of the cosine series also known, from (13), at the end of the cycle, the constant term at the end of the cycle may be evaluated using (15):

$$\frac{a_{0,ij}}{2}(1) = \left(\frac{a_{0,ij}}{2}(0) + \sum_{k=1}^{\infty} a_{k,ij}(0)\right) - \sum_{k=1}^{\infty} a_{k,ij}(1) + \int_0^1 \dot{\rho}_{ij}(\tau) d\tau. \tag{16}$$

The Fourier coefficients appear explicitly on the lhs and implicitly (through  $\dot{\rho}_{ij}$ ) on the rhs of Eqs. (13), (14), and (16). They are already cast in the following form of the nonlinear system of equations:

$$\mathbf{x} = \mathbf{g}(\mathbf{x}), \tag{17}$$



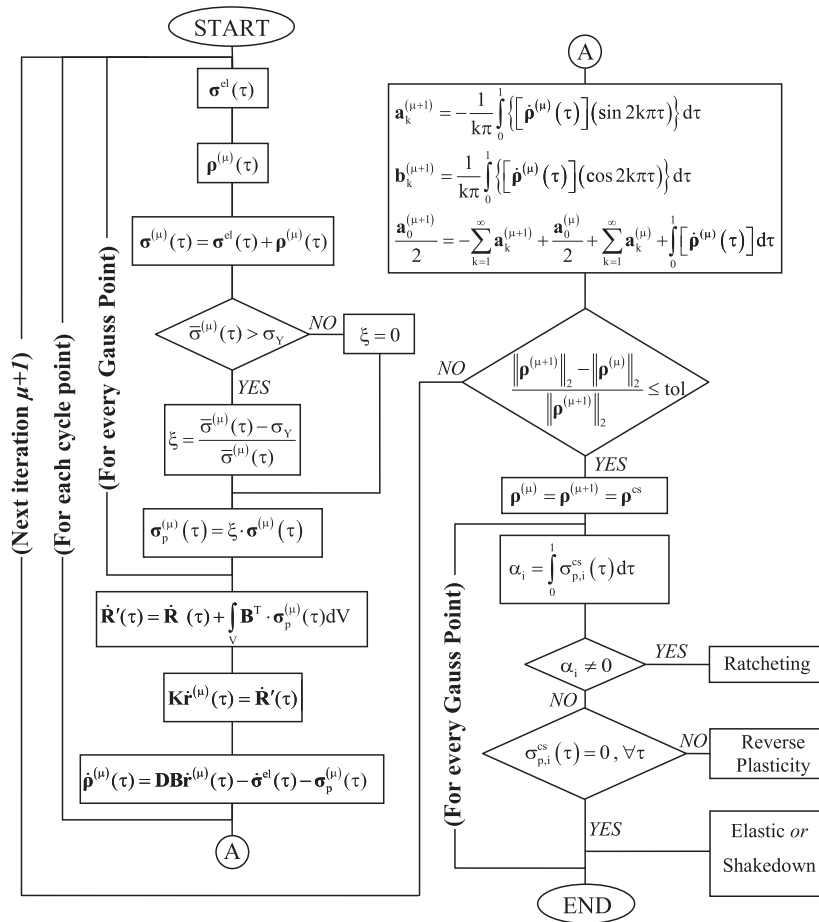


Fig. 5. Flowchart of the RSDM.

$$\alpha_i = \int_0^1 \sigma_{p,i}^{cs}(\tau) d\tau, \tag{24}$$

where  $i$  spans the components of the vector  $\sigma_p^{cs}(\tau)$ .

Three different cases may exist depending on the value of  $\alpha_i$ .

- (a) If  $\alpha_i \neq 0$ , a state of *ratcheting* exists at this GP.  
If  $\alpha_i = 0$ , we check the value  $\sigma_{p,i}^{cs}(\tau)$ .
- (b) If  $\sigma_{p,i}^{cs}(\tau) \neq 0$ , the Gauss point is in a state of *reverse plasticity*, since this must hold for pairs of cycle points of equal value but of alternating sign.
- (c) Otherwise  $\sigma_{p,i}^{cs}(\tau) = 0$ , the point has remained either *elastic* or has developed an *elastic shakedown* state.

If all the Gauss points are either elastic or in a state of elastic shakedown, then our structure under the given external loading, will also shake down. On the other hand, should sufficient GPs be in a state of ratcheting, at the steady state, our structure will undergo incremental collapse. This, numerically, may be easily manifested by the singularity of the stiffness matrix, which can be evaluated just at the end of the converged steady cycle, by zeroing the elasticity matrix  $\mathbf{D}$  at the ratcheting GPs.

### 6. Examples

Finite element programs that implement the above procedure were written for one dimensional and two dimensional structures. Results will be shown here for a three-bar truss and a holed plate

under in plane loads. A value of  $10^{-4}$  for the tolerance proved quite accurate to stop the iterations.

#### 6.1. Three bar truss

This truss structure (Fig. 6), which was analytically studied in [40], paves the way of the physical understanding of the approach.

All the elements of the truss have an equal cross sectional area of  $A = 5 \text{ cm}^2$  and are made of steel having material data of Young's modulus  $E = .21 \times 10^5 \text{ kN/cm}^2$  and a yield stress  $\sigma_y = 40 \text{ kN/cm}^2$ . The length  $L$  is taken equal to 300 cm.

A simple two node plane truss element was used to analyze the structure. The numerical procedure presented above for a continuum, was slightly altered to suit the needs of this one-dimensional stress problem. The geometry of this symmetric structure renders the residual stresses for the inclined bars 1, 3 equal to the ones of bar 2, but of opposite sign.

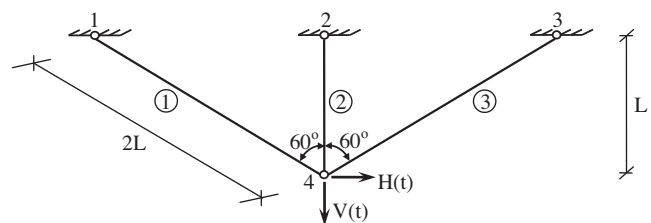


Fig. 6. Three bar truss example.

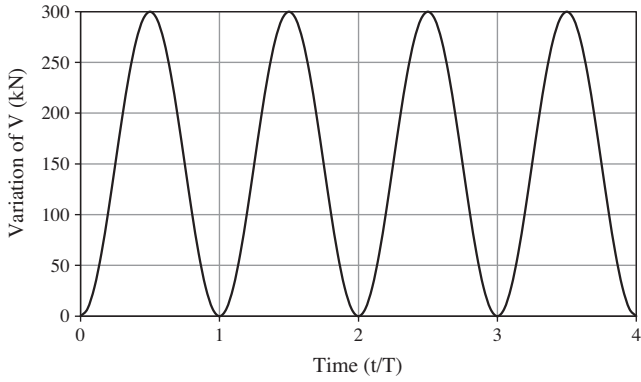


Fig. 7. Load variation with time over four periods (load case a).

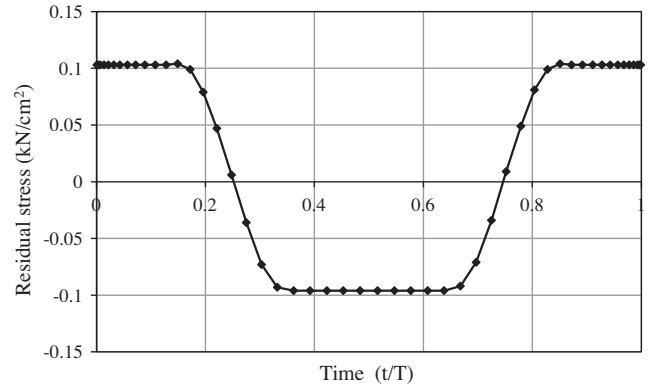


Fig. 10. Predicted steady state residual stress distribution for bar 2 inside a cycle (load case b – alternating plasticity).

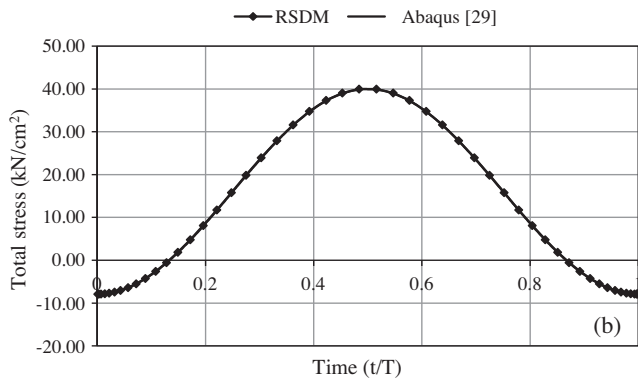
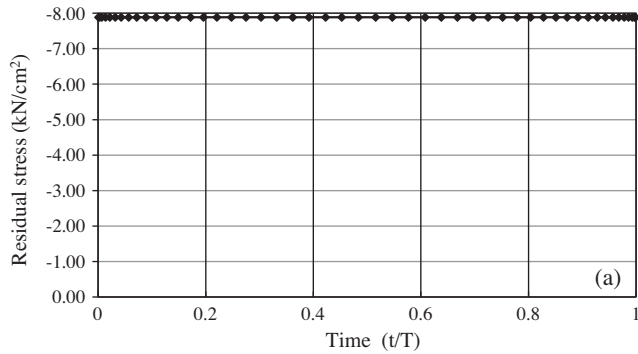


Fig. 8. Steady state stress distributions inside a cycle for bar 2 (load case a – shakedown). (a) Residual stress and (b) total stress.

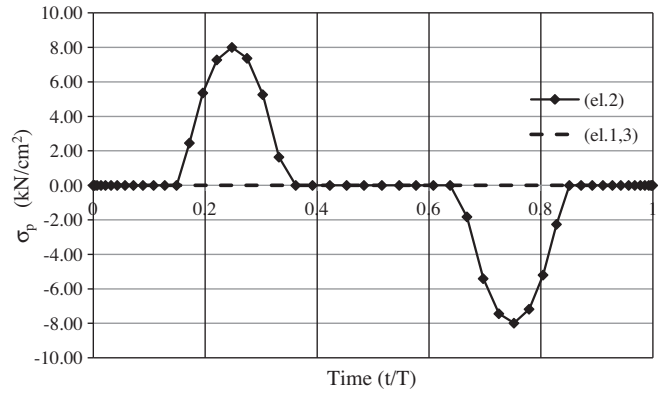


Fig. 11. Predicted  $\sigma_p^{ss}(t)$  distributions at steady state inside a cycle for all three elements (load case b – alternating plasticity).

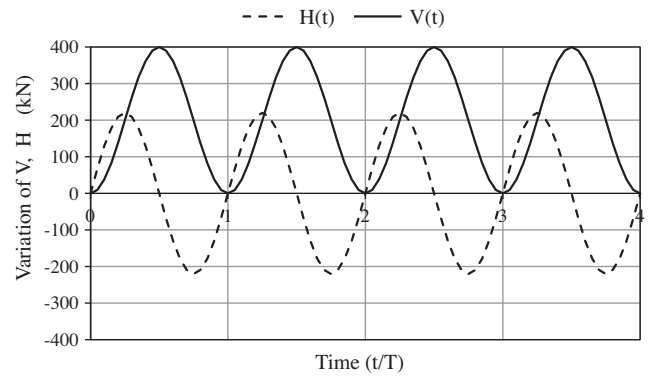


Fig. 12. Load variation with time over four periods (load case c).

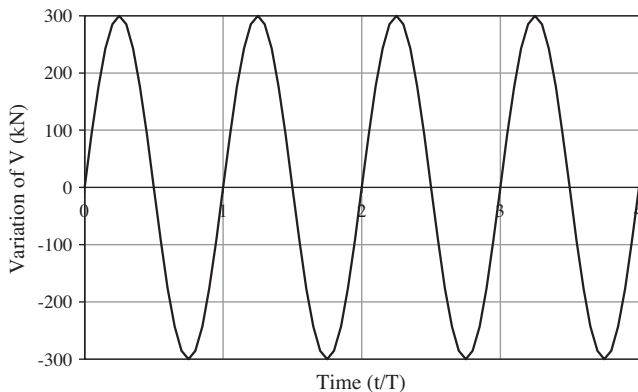


Fig. 9. Load variation with time over four periods (load case b).

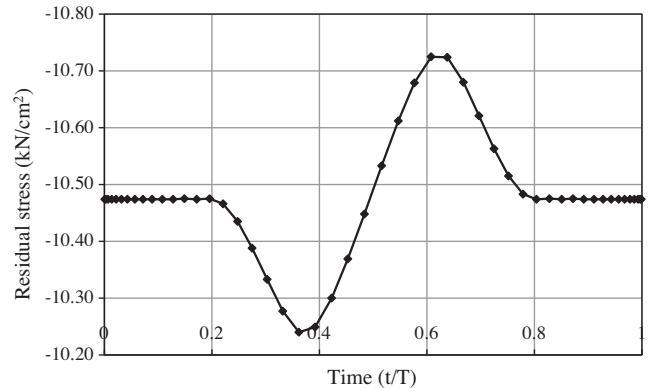


Fig. 13. Predicted steady state residual stress distribution for bar 2 inside a cycle (load case c – ratcheting).

The truss was subjected to concentrated cyclic loads  $V(t)$ ,  $H(t)$  which were applied at node 4. Three cases of loading have been considered which lead to three different cyclic steady states.

(a) The first cyclic loading case has the following variation with time (Fig. 7)

$$V(t) = 300 \sin^2(\pi t/T), \quad H(t) = 0,$$

The procedure predicts that the structure will shakedown. A confirmation of this is also provided by the computed, by the procedure, constant in time steady state residual stress (Fig. 8(a)). In Fig. 8(b) one may also see that the total stress inside the cycle nowhere exceeds the yield stress. Moreover, this stress distribution coincides with the one that was calculated from a time-stepping commercial program (Abaqus [29]), showing that the computed residual stress (Fig. 8(a)) is the actual one.

(b) The second cyclic loading case has the following variation with time (Fig. 9)

$$V(t) = 300 \sin(2\pi t/T), \quad H(t) = 0.$$

For this loading the RSDM predicts an alternating plasticity steady state. The distribution of the cyclic residual stress predicted for the middle bar inside the steady cycle may be seen in

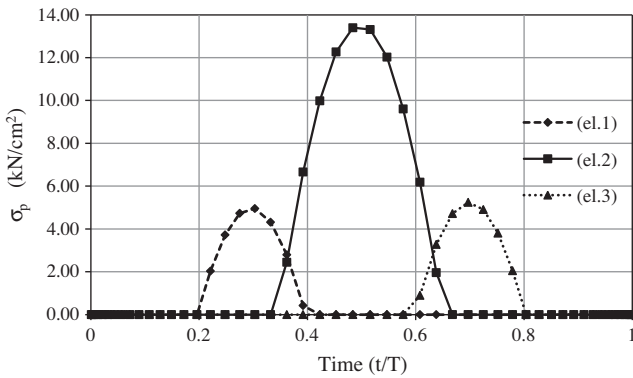


Fig. 14. Predicted  $\sigma_p^{cs}(t)$  distributions at steady state inside a cycle for all three elements (load case c – ratcheting).

Fig. 10. While the two outer bars, in the steady state, are strained only elastically, the middle bar suffers plastic strain rates, of alternating nature. These strains spread within the time intervals  $[0.149, 0.362]$  and  $[0.638, 0.851]$  inside the cycle, rendering the total plastic strain over the cycle (parameter  $\alpha_2$ -expression (24),

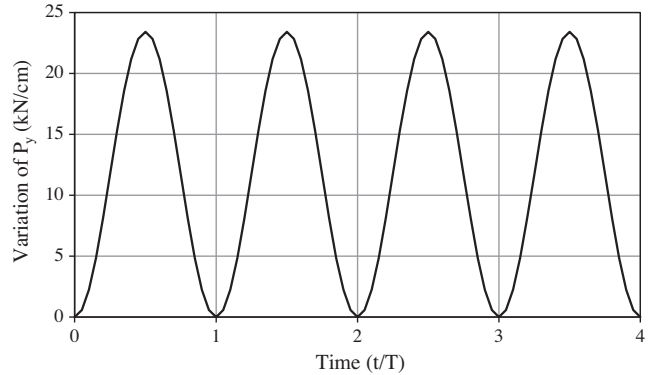


Fig. 16. Load variation with time over four periods (load case a).

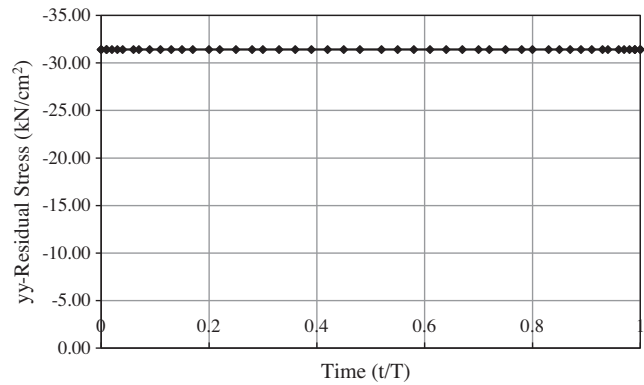


Fig. 17. Residual stress distribution at GP 2 inside a cycle at steady state (load case a – shakedown).

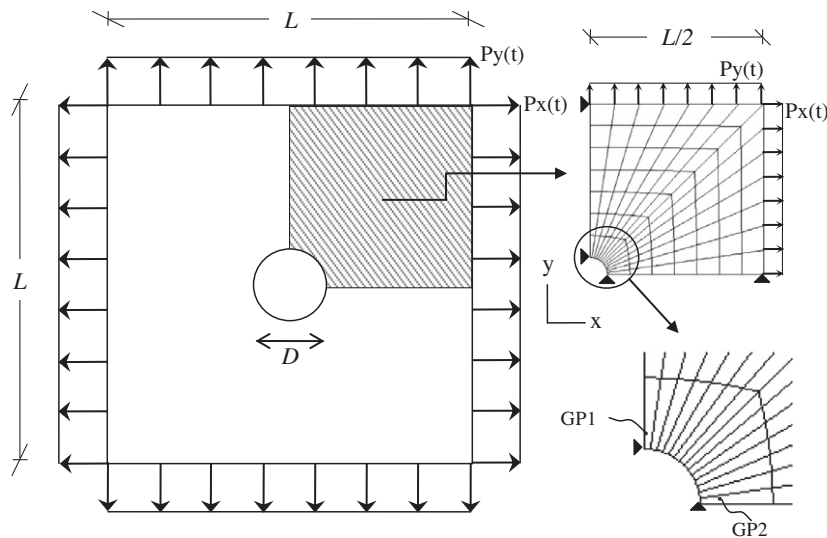
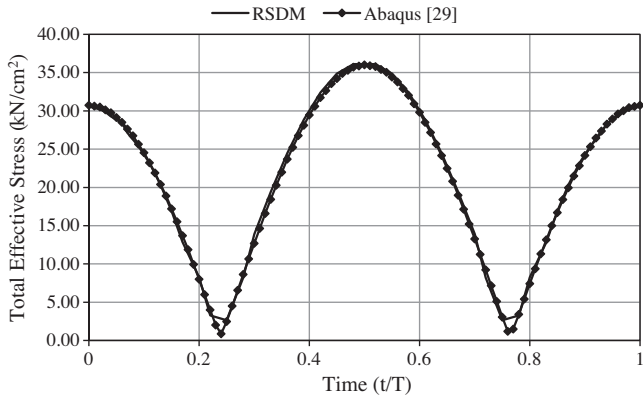


Fig. 15. The geometry, loading and the finite element mesh of a quarter of a plate.



**Fig. 18.** Effective total stress distribution at GP 2 inside a cycle at steady-state (load case a – shakedown).

also equal to the total area under the curve, Fig. 11) equal to zero.

(c) In the third cyclic loading case both the vertical and the horizontal load vary with time (Fig. 12):

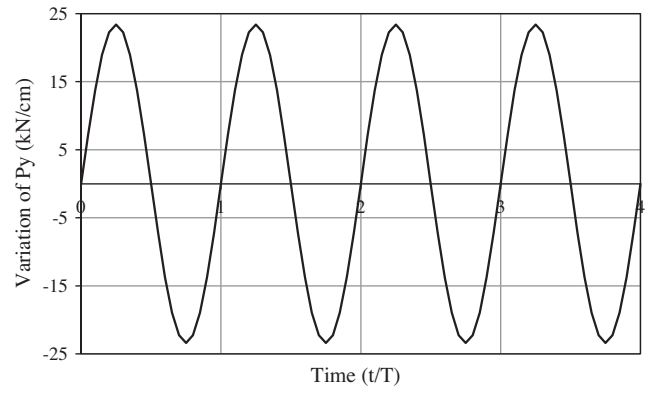


**Fig. 19.** Load variation with time over four periods (load case b).

$$V(t) = 400 \sin^2(\pi t/T), \quad H(t) = 220 \sin(2\pi t/T).$$

The variation of the predicted steady state residual stress inside a cycle for the middle bar may be seen in Fig. 13.

The values of the parameters  $\alpha_i$ ,  $i = 1, 2, 3$ , for all the three bars, turn out to be different than zero. This loading case will lead the

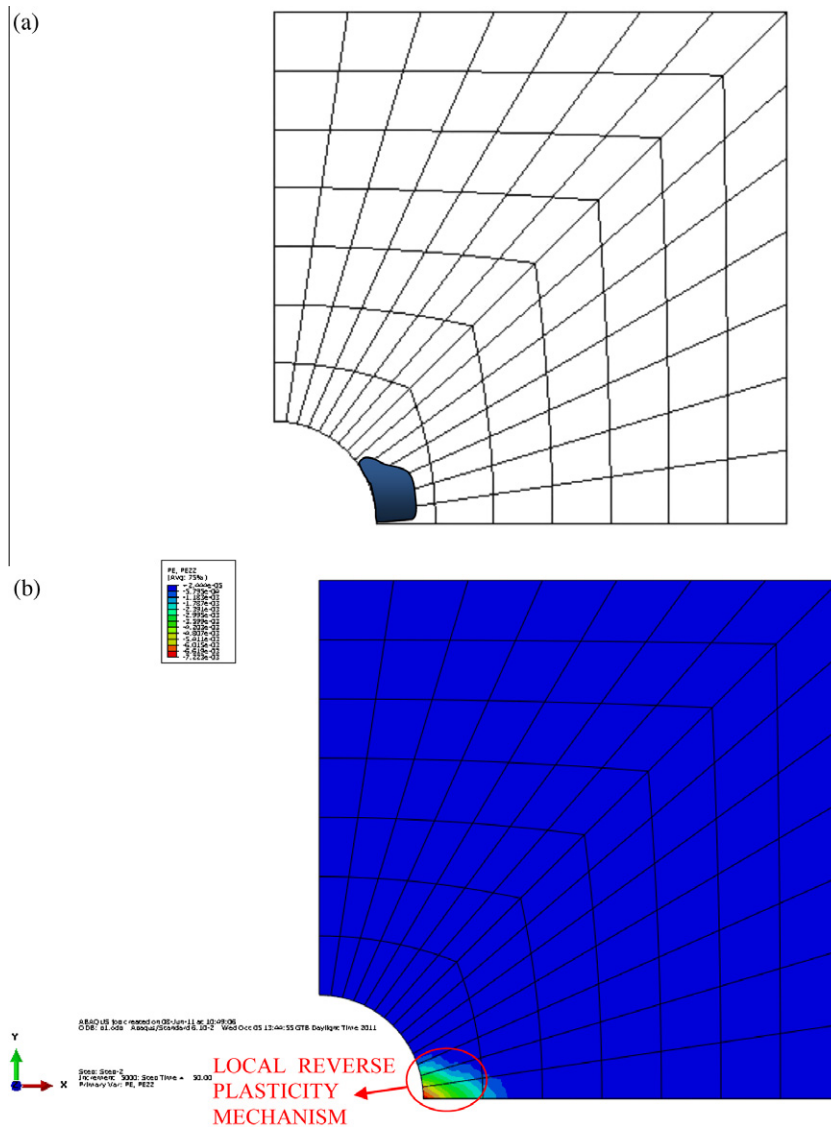


**Fig. 20.** Local alternating plasticity mechanism for load case b. (a) RSDM and (b) Abaqus [29].

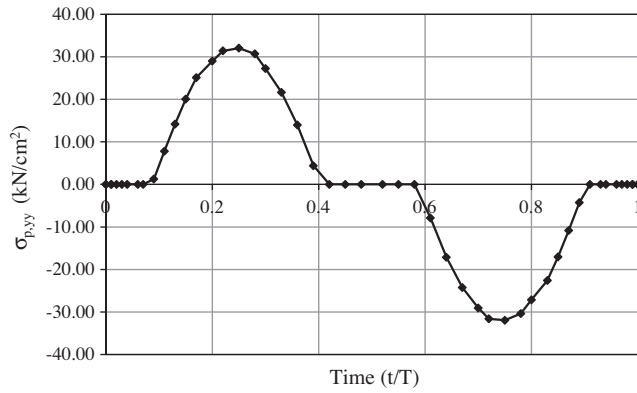


Fig. 21. Predicted cyclic steady-state distributions of the yy component of the stress vector  $\sigma_p^{cs}$  at GP 2 (load case b – alternating plasticity).

structure to ratcheting, since the non simultaneous plasticization of all the bars inside the steady cycle (Fig. 14) constitutes an incremental collapse mechanism.

6.2. Square plate with a circular hole

The second example of application is a benchmark example, and is a plane stress problem of a square plate having a circular hole in its middle. The loading is applied in equal pairs along the edges of the plate (Fig. 15). Due to the symmetry of the structure and the loading, we only analyze one quarter of the plate. The geometry of the plate and its finite element mesh are shown in Fig. 15. The ratio between the diameter  $D$  of the hole and the length  $L$  of the plate is equal to 0.2. Also the ratio of the depth of the plate to the length  $L$  is equal to 0.05. The plate is made of steel with the following material data: Young’s modulus  $E = .21 \times 10^5$  kN/cm<sup>2</sup>, Poisson’s ratio  $\nu = 0.3$  and yield stress  $\sigma_y = 36$  kN/cm<sup>2</sup>. The above geometrical and material data are the same as the ones used in [22].

A case of  $L = 20$  cm has been chosen herein. The finite element mesh used consists of 98, eight-noded, isoparametric elements with  $3 \times 3$  Gauss integration points.

The various loading cases, used, were taken so as to belong to different regions below and above shakedown and ratcheting boundaries, as these have been estimated in [22]. Results are plotted for the most highly stressed points, which depending on the loading case, are either GP 1 or GP 2, the Gauss points closest to the cusps of the hole (Fig. 15).

(a) The first cyclic loading case has the following variation with time (Fig. 16):

$$P_y(t) = 0.65\sigma_y \sin^2(\pi t/T), \quad P_x(t) = 0.$$

In Fig. 17 the computed by the RSDM steady-state residual stress distribution is plotted for the GP 2.

The stress distribution is the actual stress distribution as this may be confirmed in Fig. 18, where the results of the time stepping program [29] coincide with the results of the RSDM. The steady state predicted for the structure, by the procedure, is a shakedown state and this complies with the fact that this loading is below the shakedown boundary estimated in [22].

(b) The second cyclic loading case has the following variation with time (Fig. 19):

$$P_y(t) = 0.65\sigma_y \sin(2\pi t/T), \quad P_x(t) = 0.$$

The value of this load, at many cycle points, proves to be well in excess of the shakedown-reverse plasticity boundary, plotted in [22]. The present numerical procedure (RSDM) also shows that this loading will lead some GPs to local reverse plasticity. In Fig. 20(a) one may see the local reverse plasticity mechanism predicted by the RSDM, which compares well with the time-stepping program [29] that also predicts such a mechanism (Fig. 20(b)).

If we compare the values of the components of the excess vector  $\sigma_p^{cs}$  at GP 2, which is the most highly strained Gauss point of the structure, we conclude that the most plastically strained direction is yy. The variation of this component inside the cycle is plotted in Fig. 21. We may see that plastic straining occurs, alternately, inside the time intervals [0.06,0.42] and [0.58,0.91] at the steady cycle. At the same time, one may observe (Fig. 22) the fluctuation around zero of the plastic strain along the yy direction for the first 50 cycles at this GP of the time stepping program [29].

(c) The third cyclic loading case involves two loads, one constant in time and one varying with time (Fig. 23):

$$P_x = 0.6\sigma_y = const, \\ P_y(t) = 0.8\sigma_y \sin^2(\pi t/T).$$

The combination of the two loads leads to an excursion well above the shakedown-reverse plasticity boundary established in [22]. An alternating plasticity condition is also predicted by the present numerical procedure (RSDM) for some GPs near the edge of the hole (Fig. 24(a)). A very good match of this mechanism is observed with the one found by Abaqus [29] (see Fig. 24(b)). Once again the most

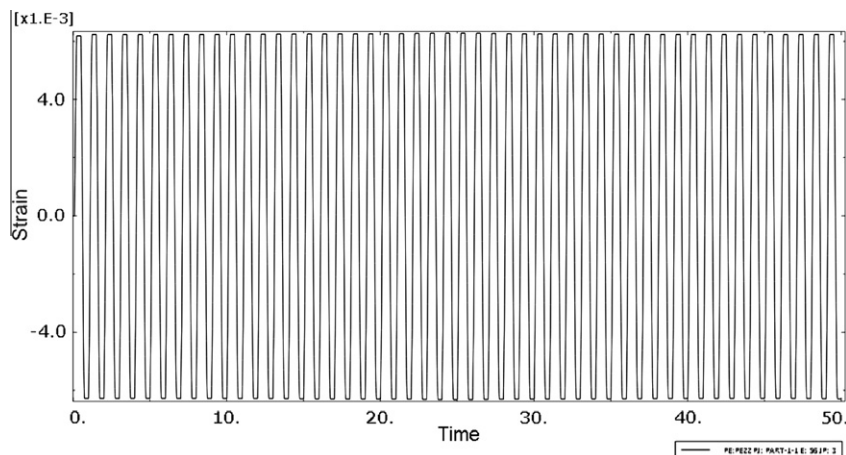


Fig. 22. Abaqus [29] yy-plastic strain variation over the first 50 cycles at the GP 2 (load case b – alternating plasticity).

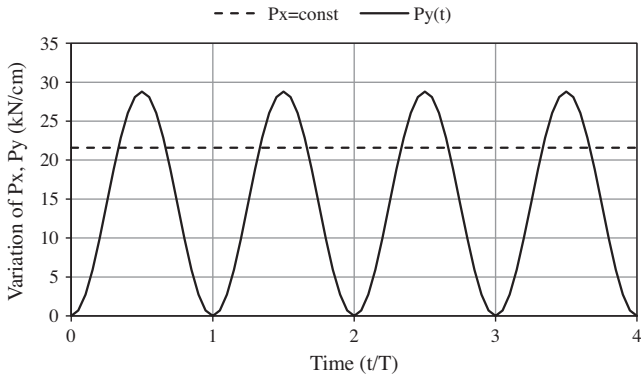


Fig. 23. Load variation with time over four periods (load case c).

strained GP is GP 2, and the most plastically strained direction is again yy. Plotting the variation of this component of  $\sigma_p^{cs}$  (Fig. 25), we may see that plastic straining of alternating nature occurs inside

the time intervals [0, 0.09], [0.39, 0.61] and [0.91, 1] at the steady cycle. One may now compare the results of a time-stepping program [29] (Fig. 26). Looking at the plotting of the plastic strains over the first 100 cycles, one may see that for this loading we have alternating plastic strains around a non-zero value. The pattern of this straining does not seem to change as we approach 1000 cycles, although the mean value drops, thus making it difficult to decide whether the cumbersome time-stepping program has reached a steady state solution.

(d) The fourth cyclic loading case also involves two loads, one constant in time and one varying with time (Fig. 27).

$$P_x = 0.85\sigma_y = \text{const},$$

$$P_y(t) = 0.5\sigma_y \sin^2(\pi t/T).$$

This loading, at many cycle points, is above the ratcheting boundary of [22].

In Fig. 28 one may see the convergence of the RSDM for this loading case. The uniform convergence of the RSDM is typical for

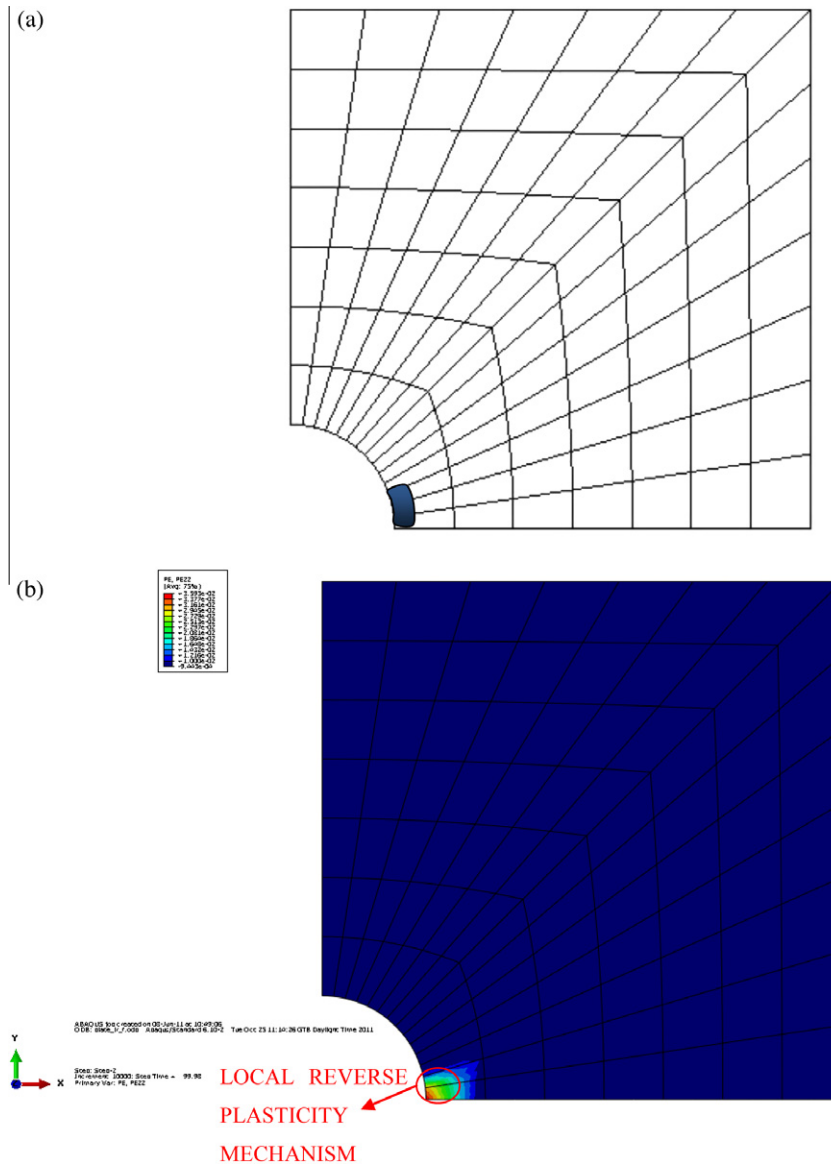


Fig. 24. Local alternating plasticity mechanism for load case c. (a) RSDM and (b) Abaqus [29].

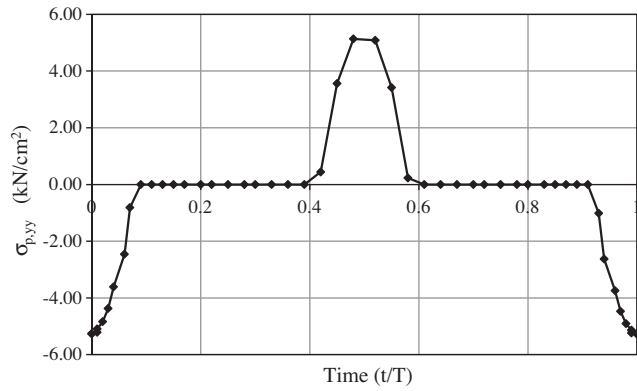


Fig. 25. Predicted cyclic steady-state distributions of the yy component of the stress vector  $\sigma_p^{cs}$  at GP 2 (load case c – alternating plasticity).

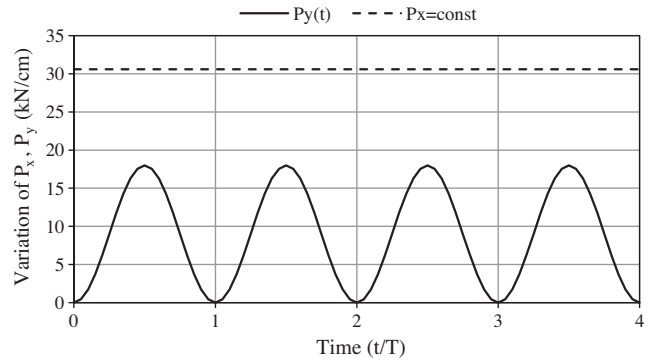


Fig. 27. Load variation with time over four periods (load case d).

all the loading cases that were considered before, with the present one requiring the biggest number of iterations.

The results for the most strained GP 1 may be seen in Fig. 29, where plastic straining of the same positive sign inside the cycle intervals [0,0.22] and [0.78, 1] at the steady cycle is observed. Here we plot the xx direction of  $\sigma_p^{cs}$  which corresponds to the largest plastic straining among the three components. This ratcheting behavior holds also for quite a few GPs around the structure, with the higher straining (the GPs with the parameters  $\alpha_i$ 's having the bigger values) within the region marked in Fig. 30(a), which definitely constitutes an incremental collapse mechanism. This mechanism is also confirmed by the time-stepping program ([29]) which diverges after the 47th cycle; at this point, the appearance of the plastically most highly strained region of the time-stepping program (Fig. 30(b)) matches closely the one predicted by the present procedure (as shown in Fig. 30(a)).

The number of time points inside the cycle should be enough so that it may adequately represent the applied loading. On the other hand, for an alternating plasticity case, it may be useful to increase the time points so that the values of the parameters  $\alpha_i$ 's (Eq. (24)) approach zero within a small tolerance.

Fifty time points inside the cycle were used for all the examples considered herein. For the cases of alternating plasticity, the use of 200 points decreased the values of the parameters  $\alpha_i$ 's by an order of magnitude.

The RSDM proved to be quite stable, no matter which asymptotic behavior was reached. Three terms of the Fourier series were

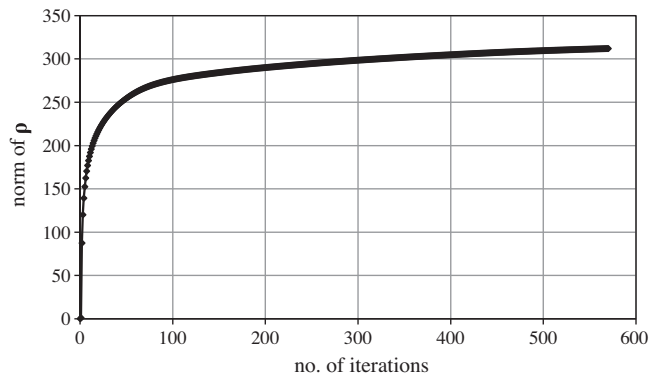


Fig. 28. Convergence of the iterative procedure (load case d).

found enough to represent the residual stress distribution. Computational efficiency, apart from the small number of the Fourier coefficients, is further enhanced due to the fact that the stiffness matrix needs to be decomposed only once in the beginning of the procedure. Thus, within the adopted tolerance, the number of the iterations ranged from a minimum of 20 for the case of ratcheting of the truss example, to a maximum of 570 for the case of ratcheting of the plate example. The amount of CPU-time required to solve this last case was just 136 s, for an Intel Core i7 at 2.93 GHz with 4096 MB RAM.

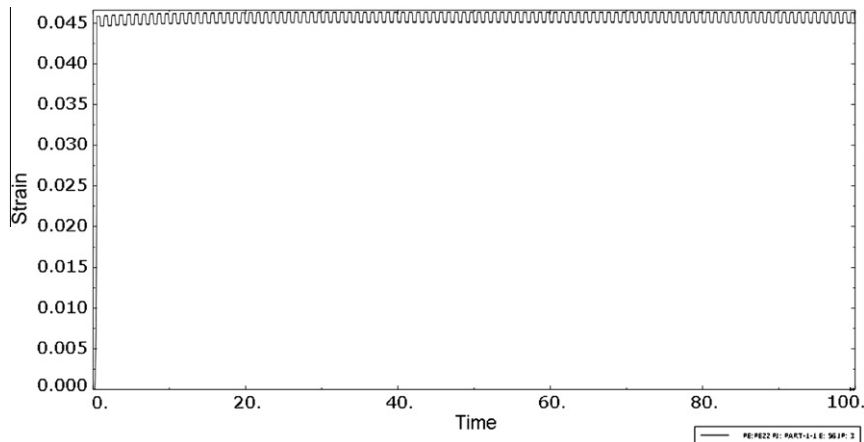
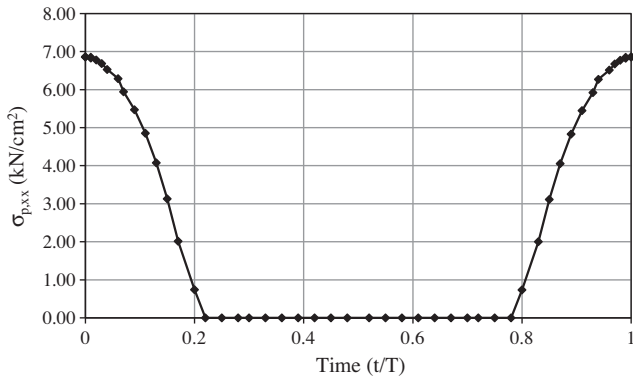


Fig. 26. Abaqus [29] yy-plastic strain variation at the GP 2 over the first 100 cycles (load case c – alternating plasticity).



**Fig. 29.** Predicted cyclic steady-state distributions of the xx component of the stress vector  $\sigma_p^{xx}$  at GP 1 (load case d – ratcheting).

**7. Conclusions**

This work presents a method, named RSDM, which predicts whether the continuous application of a given cyclic load would lead an elastoplastic structure either to safety or to low cycle

fatigue or to excessive inelastic deformations, without having to resort to cumbersome time-stepping calculations. The method can be classified as a Direct Method in the sense that it addresses, directly, the properties of the steady state cycle. The basis of the method is the cyclic nature of the residual stress in the steady cycle. Therefore, following its decomposition in Fourier series, the residual stress distribution in the steady cycle is approached through a computational procedure that approximates the Fourier coefficients in an iterative manner. Plasticity effects may be easily implemented by a radial return on the yield surface along the total stress vector, which is the sum of a purely elastic solution and the residual stress. After convergence, if the applied loading is within the shakedown boundary, the evaluated residual stress, constant in time inside the cycle, coincides with the actual residual stress. If the loading, on the other hand, is above the shakedown boundary, the evaluated residual stress renders a steady state total stress, which is unsafe. The integral of the plastic straining over the cycle of loading, in the unsafe regions, determines whether we have regions of alternating plasticity or ratcheting. In the latter case, the procedure checks whether the structure itself will suffer incremental collapse. The whole approach proved to be numerically stable and computationally efficient.

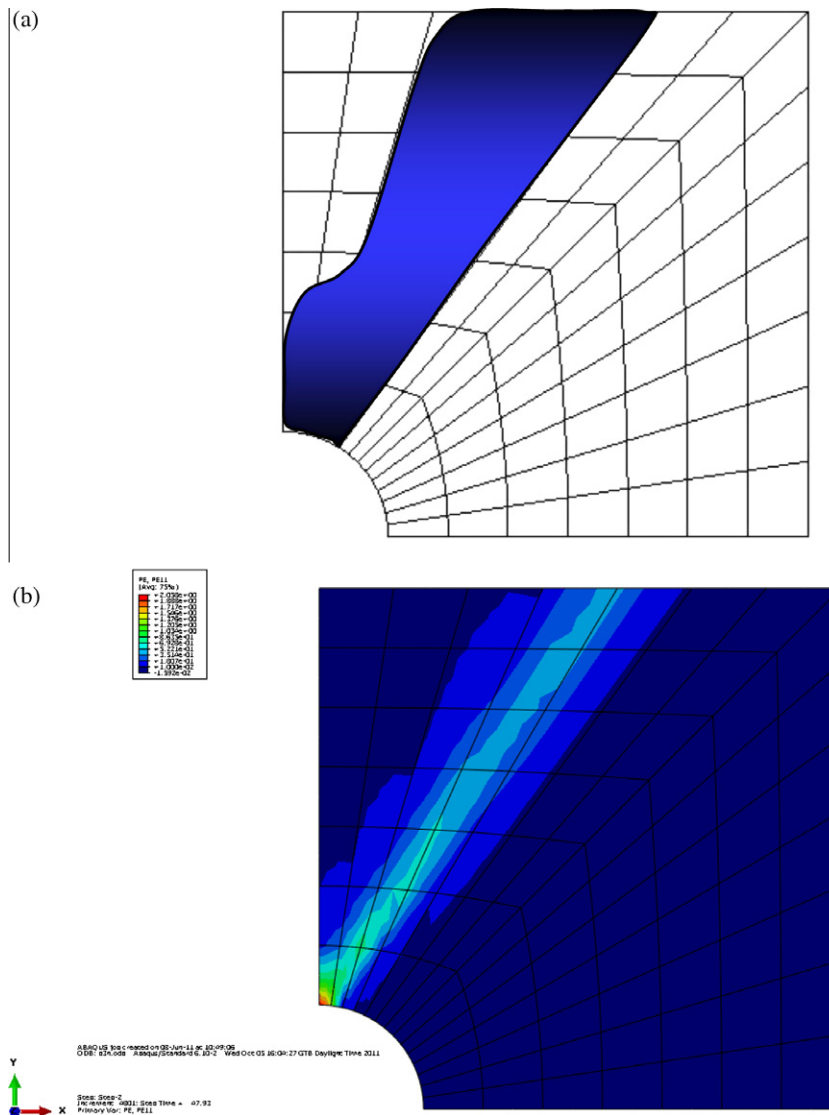


**Fig. 30.** Ratcheting mechanism for load case d. (a) RSDM and (b) Abaqus [29].

The proposed simple way of assessing the plastic effects makes possible to use any other yield surface except for the von Mises yield surface which was used herein for the numerical examples presented.

Comparing the RSDM with the existing DCA, one may note that with the DCA, plastic strains over the cycle are estimated in an incremental way. Iterations lead the plastic strain distribution to a steady state which, due to the assumptions of the method, can only be an alternating plasticity steady state. On the other hand, the RSDM is simpler, since it is a pure iterative method. It is also more general, as it may predict any steady state, either alternating plasticity or incremental collapse.

The procedure was developed for an elastic–perfectly plastic material. It may be extended to account for different material behaviors (like hardening, etc.)

The method assumes the complete knowledge of the loading history inside the cycle. Nevertheless, it appears to have the potential to provide also safety margins for any cyclic history in a given loading domain and work is being done towards this direction.

### Acknowledgements

Financial support for this work, for the second author, was provided by the “Propondis” and the “Onassis” foundations. Their support is gratefully acknowledged.

### References

- [1] D.C. Drucker, A definition of stable inelastic material, *ASME J. Appl. Mech.* 26 (1959) 101–106.
- [2] E. Melan, Zur plastizität des räumlichen Kontinuums, *Ing. Arch.* 9 (1938) 116–126.
- [3] W. Koiter, in: I.N. Sneddon, R. Hill (Eds.), *General Theorems for Elastic–Plastic Solids*, North-Holland, Amsterdam, 1960.
- [4] G. Maier, A shakedown matrix theory allowing for workhardening and second-order effects, in: *Proceedings of the Symposium on Foundations of Plasticity*, Warsaw, 1972.
- [5] L. Corradi, G. Maier, Dynamic non-shakedown theorem for elastic perfectly plastic continua, *J. Mech. Phys. Solids* 22 (1974) 401–413.
- [6] G. Cocchetti, G. Maier, Static shakedown theorems in piecewise linearized poroplasticity, *Arch. Appl. Mech.* 68 (1998) 651–661.
- [7] N. Zouain, L. Borges, J.L. Silveira, An algorithm for shakedown analysis with nonlinear yield function, *Comput. Methods Appl. Mech. Engrg.* 191 (2002) 263–2481.
- [8] D.K. Vu, A.M. Yan, H. Nguyen-Dang, A primal-dual algorithm for shakedown analysis of structures, *Comput. Methods Appl. Mech. Engrg.* 193 (2004) 4663–4674.
- [9] T.N. Tran, G.R. Liu, H. Nguyen-Xuan, T. Nguyen-Thoi, An edge-based smoothed finite element method for primal-dual shakedown analysis of structures, *Int. J. Numer. Methods Engrg.* 82 (2010) 917–938.
- [10] J.-W. Simon, D. Weichert, Numerical lower bound shakedown analysis of engineering structures, *Comput. Methods Appl. Mech. Engrg.* 200 (2011) 2828–2839.
- [11] C.D. Bisbos, A. Makrodimitopoulos, P.M. Pardalos, Second-order cone programming approaches to static shakedown analysis in steel plasticity, *Optimiz. Methods Softw.* 20 (2005) 25–52.
- [12] A.D. Nguyen, A. Hachemi, D. Weichert, Application of the interior point method to shakedown analysis of pavements, *Int. J. Numer. Methods Engrg.* 4 (2008) 414–439.
- [13] G. Garcea, L. Leonetti, A unified mathematical programming formulation of strain driven and interior point algorithms for shakedown and limit analysis, *Int. J. Numer. Methods Engrg.* 88 (2011) 1085–1111.
- [14] J. Zarka, J.J. Engel, G. Inglebert, On a simplified inelastic analysis of structures, *Nucl. Engrg. Des.* (1980) 333–368.
- [15] J. Zarka, J. Frelat, G. Inglebert, P. Kasmal-Navidi, *A New Approach to Inelastic Analysis of Structures*, Martinus Nijhoff Pub., Dordrecht, 1990.
- [16] A.R.S. Ponter, K.F. Carter, Shakedown state simulation techniques based on linear elastic solutions, *Comput. Methods Appl. Mech. Engrg.* 140 (1997) 259–279.
- [17] D. Mackenzie, T. Boyle, A method of estimating limit loads by iterative elastic analysis. I: Simple examples, *Int. J. Press. Vess. Piping* 53 (1993) 77–95.
- [18] D. Mackenzie, J.T. Boyle, R. Hamilton, The elastic compensation method for limit and shakedown analysis: a review, *J. Strain Anal.* 35 (2000) 171–188.
- [19] A.R.S. Ponter, P. Fuschl, M. Engelhardt, Limit analysis for a general class of yield conditions, *Eur. J. Mech. A/Solids* 19 (2000) 401–421.
- [20] A.R.S. Ponter, M. Engelhardt, Shakedown limits for a general yield condition: implementation and application for a von Mises yield condition, *Eur. J. Mech. A/Solids* 19 (2000) 423–445.
- [21] A.R.S. Ponter, H. Chen, A minimum theorem for cyclic load in excess of shakedown, with application to the evaluation of a ratchet limit, *Eur. J. Mech. A/Solids* 20 (2001) 539–553.
- [22] H.F. Chen, A.R.S. Ponter, A method for the evaluation of a ratchet limit and the amplitude of plastic strain for bodies subjected to cyclic loading, *Eur. J. Mech. A/Solids* 20 (2001) 555–571.
- [23] J. Ure, H. Chen, T. Li, W. Chen, D. Tipping, D. Mackenzie, A direct method for the evaluation of lower and upper bound ratchet limits, *Procedia Engrg.* 10 (2011) 356–361.
- [24] R. Adisi-Asl, W. Reinhardt, Non-cyclic shakedown/ratcheting boundary determination. Part 1: Analytical approach, *Int. J. Press. Vess. Piping* 88 (2011) 311–320.
- [25] R. Adisi-Asl, W. Reinhardt, Non-cyclic shakedown/ratcheting boundary determination. Part 2: Numerical implementation, *Int. J. Press. Vess. Piping* 88 (2011) 321–329.
- [26] J. Abou-Hanna, T.E. McGreevy, A simplified ratcheting limit method based on limit analysis using modified yield surface, *Int. J. Press. Vess. Piping* 88 (2011) 11–18.
- [27] D.A. Gokhfeld, O.F. Cherniavsky, *Limit Analysis of Structures at Thermal Cycling*, Sijthoff & Noordhoff, 1980.
- [28] M.H. Maitournam, B. Pommier, J.-J. Thomas, Détermination de la réponse asymptotique d’une structure anélastique sous chargement thermomécanique cyclique, *CR Mec.* 330 (2002) 703–708.
- [29] Abaqus 6.10, *Theory & User’s manual*, Dassault Systèmes, 2010.
- [30] K.V. Spiliopoulos, Simplified methods for the steady state inelastic analysis of cyclically loaded structures, in: D. Weichert, G. Maier (Eds.), *Inelastic Analysis of Structures under Variable Loads*, Kluwer Academic Publishers, 2000, pp. 213–232.
- [31] K.V. Spiliopoulos, A simplified method to predict the steady cyclic stress state of creeping structures, *ASME J. Appl. Mech.* 69 (2002) 149–153.
- [32] C.O. Frederick, P.J. Armstrong, Convergent internal stresses and steady cyclic states of stress, *J. Strain Anal.* 1 (1966) 154–169.
- [33] C. Polizzotto, Variational methods for the steady state response of elastic-plastic solids subjected to cyclic loads, *Int. J. Solids Struct.* 40 (2003) 2673–2697.
- [34] J.A. König, *Shakedown of Elastic–Plastic Structures*, Elsevier, Amsterdam, 1987.
- [35] G.P. Tolstov, *Fourier Series*, Dover, New York, 1962.
- [36] E. Isakson, H.B. Keller, *Analysis of Numerical Methods*, J. Wiley, 1966.
- [37] R.D. Cook, D.S. Malkus, M.E. Plesha, R.J. Witt, *Concepts and Applications of Finite Element Analysis*, J. Wiley & Sons, 2002.
- [38] E.A. de Souza Neto, D. Peric, D.R.J. Owen, *Computational Methods for Plasticity: Theory and Applications*, J. Wiley, Chichester, 2008.
- [39] J.C. Simo, T.J.R. Hughes, *Computational Inelasticity*, Springer, 1998.
- [40] J.B. Martin, *Plasticity*, MIT Press, 1975.